ISSN 0018-151X, High Temperature, 2010, Vol. 48, No. 6, pp. 903–909. © Pleiades Publishing, Ltd., 2010.
Original Russian Text © V.V. Golub, A.S. Saveliev, V.A. Sechenov, E.E. Son, D.V. Tereshonok, 2010, published in Teplofizika Vysokikh Temperatur, 2010, Vol. 48, No. 6, pp. 948–955.

HEAT AND MASS TRANSFER AND PHYSICAL GASDYNAMICS

Plasma Aerodynamics in a Supersonic Gas Flow

V. V. Golub[a], A. S. Saveliev[b], V. A. Sechenov[b], E. E. Son[a, b], and D. V. Tereshonok[a, b]

[a] *Joint Institute for High Temperatures, Russian Academy of Sciences, ul. Izhorskaya 13, building 2, Moscow, 125412 Russia*

[b] *Moscow Institute of Physics and Technology (State University), Dolgoprudny, Institutskii per. 9, Moscow oblast, 141700 Russia*

Received July 16, 2010

Abstract—We perform an experimental study and numerical simulation of the process of periodic initiation of spark extended discharge in air flow with a Mach number $M = 2$. Critical parameters of the discharge are measured in a high velocity air flow, and visualization of the gas flow in the presence of the discharge is performed. The influence of the discharge on the flow near the body surface streamlined by the supersonic flow is studied.

DOI: 10.1134/S0018151X10060180

INTRODUCTION

At present, the aerodynamics of aircraft based on the geometry of their parts is close to perfect. The direction of improving the wing profile and other aircraft components due to geometry has been practically exhausted. Therefore, at present more efforts of scientists and engineers are spent on application of new promising methods for improving the picture of air flow around the surface of an aircraft, so-called active control methods. The first attempts at applying these devices were microelectromechanical systems (MEMS technologies), technologies and devices combining microelectronic and micromechanical components. In aerodynamics these devices are applied as mechanical oscillators and vortex generators.

Another type of promising devices for gas flow control is plasma actuators. The main idea in this case is that electric discharge of different types is created in the gas (air) flow and the flow acquires additional parameters, for example, enthalpy due to additional acceleration of partially ionized gas in the strong electric field or due to gas heating. The main applied discharge types are corona, spark, dielectric barrier, and microwave. Unlike mechanical actuators, plasma devices can be used to input into the incident gas flow a nearly unlimited amount of energy, and the operation speed of these devices is comparable with that of MEMS devices. It should be noted that the development of plasma aerodynamics is accompanied by rapid development of semiconductor electronics and technologies of electric energy conversion. It should be noted that plasma aerodynamics, the field of aerodynamics in which new methods of active influence on the gas flow using plasma technologies, considers both external and internal aerodynamics. Devices for plasma creation near the surface streamlined by the subsonic or supersonic air are useful in designing new types of engines (including supersonic direct-flow ones) and MHD generators.

While at present different types of electric discharges are used for controlling subsonic gas flow, only some of them are applicable to a supersonic gas flow. This is connected with the fact that at rather high velocities of the incident flow, ionization travels in a different way, supersonic flow carries away part of ions from the region of strong electric field, and the discharge intensity and energy input decrease. For example, it was shown that dielectric barrier discharge can substantially influence the picture of subsonic flow with a velocity up to 100 m/s [1]. In the transonic air flow, no influence of this type of discharge on the flow is observed [2]. In a supersonic air flow with a Mach number $M = 2$, the flow strongly changes the plasma structure near the actuator [3]. A more promising method of influencing the parameters of the supersonic air flow is pulsed-periodic action, for example, using high current spark discharge; in this case, the mechanism of discharge action on the flow is thermal. One of the methods for creating such perturbation is the application of gas heating discharge, which results in thermal perturbation. It was theoretically shown in [10] that heat supply in the gas flow results in the formation of vortices; therefore, for understanding the physical basics of gas motion control using thermal action, the interaction of the formed vortices with the incident flow should be studied. Such studies were begun in a number of papers [6–9]. These papers studied the heating laminar boundary layer for the incident flux with a Mach number $M = 1.5$. The evolution of the pair of formed vortices upon their downward motion along the flow was analyzed. The results have

much in common with direct numerical simulation performed in [11] for mechanical perturbation. Experimental papers on investigation of the influence of spark discharge on the picture of supersonic flow in the presence of an oblique shock wave and separated zone are also known [12, 13].

Comparison of mechanical and thermal impact gives certain conclusions on the quality of the flow control. Although mechanical devices can be efficient, they have certain disadvantages, namely, complex design, large weight, noncompact character; they can result in undesirable vibrations and consist of mechanical parts that can wear out or break. The main advantages of thermal and plasma actuators are reliability, simplicity, low energy consumption, and the possibility of control with high frequencies corresponding to the Strouhal number in a flow on the order of unity, for which the action on the flow is most efficient.

EXPERIMENTAL STUDIES

In this study, we consider the possibility of initiating an extended spark discharge with a frequency on the order of kHz in a supersonic air flow with a Mach number $M = 2$. A sectioned discharger with a characteristic distance between the electrodes on the order of 10 cm (model size) is used as the plasma actuator, an electric device that creates the plasma in a flow for controlling the flow regime. The flow parameters for which extended spark discharge can be initiated [4] were already obtained earlier; however, in that study, the process of single discharge initiation with energies much higher than 1 J in the flow behind the shock wave front was considered. Of practical interest is the process of initiation pulsed-periodic discharge with a period comparable to the flight time of the flow above the considered part of the body, i.e., a frequency in the kilohertz range. In this case, the Strouhal number in the physical process is about 1.

The process of generating an extended spark discharge was studied using a supersonic atmospheric–vacuum wind tunnel with a flow Max number $M = 2$ (flow velocity $V = 520$ m/s), Reynolds number of about 10^6, and static pressure in the flow $p = 0.15$–0.18 atm. An aerodynamic model with a curvilinear surface and the plasma actuator embedded in it so that the body surface was smooth were situated behind the output cross section of the de Laval nozzle. A NACA64a212 profile made from a dielectric material (quartz) with a characteristic size of 10 cm was used as the aerodynamic model. The size of the profile chord was constant in all cross sections of the profile; therefore, the model streamline was considered two-dimensional. The sealed working chamber of the wind tube into which supersonic air flow was input is equipped with optical glass for visualization of the flow in the presence of electric discharge. Flow visualization was performed with an IAB-451 shadow device using the Toepler method (knife and slit) [5], and the shadow method. The studied flow region was backlit by a DK Hadjustable SSh-150-1 arc xenon lamp. The Schlieren or shadow picture of the flow was recorded using a Photron FASTCAM SA4 high-speed digital camera with a resolution of 1024 × 1024 pixels, an exposure time of not lower than 1 μs, and a shooting rate of up to 20 000 frames/s. The aerodynamic profile was placed in the working chamber in such a way that the generatrices of the streamlined surface were parallel to the optical axis of the shadow device and the front edge of the profile was perpendicular to the axis of the de Laval nozzle. The working chamber was equipped with a mechanical device for changing the angle of attack of the profile with respect to the incident flow. When the angle of attack was changed, the orientation of the profile with respect to the optical axis of the shadow device and the nozzle axis were retained. A SPELLMAN SL15P2000 high voltage source with an adjustable voltage of 0–15 kV and a maximum output power of 2 kW was used to power the actuator. The schematic diagram of discharge initiation in the frequency regime consists of the ballast resistance R, whose value is determined by the maximal output current of the high voltage source for the given voltage, and a set of K15-5-type high voltage ceramic condensers with a capacity $C = 4.7$ nF. Since the nominal tolerance of the condenser is large, before the experiment, the total capacity was additionally measured (measurement precision 4%). The characteristic resistance is $R = 100$ kΩ. The condenser charging time is on the order of RC, and this quantity determines the frequency of discharge initiation in the flow. The electric parameters of the discharge were measured using a LeCroy WaveRunner 104Xi digital oscilloscope, the voltage at the discharger was measured using a Tektronix P6015A 1 : 1000 divider, and the front of the discharge current was recorded using a Rogowski coil.

Experiments on streamlining with and without a discharge on the body surface were performed for the fully expanded regime for a uniform profile of the supersonic flow velocity. The angle of attack of the aerodynamic profile was varied from 0 to 15 deg with respect to the incident flow. Experiments on schlieren visualization of the flow showed that in this range of angles of attack, the separated flow is forms near the back edge of the profile. For the fully expanded regime of wind tube operation, the separation is most pronounced for an angle of attack of 12 deg; it is situated at a distance of 30–50 mm from the back edge above the surface of the NACA profile. Therefore, at a distance of 40 mm from the back edge, the actuator was embedded into the surface for creating spark discharge and investigating the influence of pulsed gas heating on the flow picture. Experimental studies showed that for discharge initiation frequencies of about 6 kHz and an average input power of 500 W per 10 cm, the quality of the profile surface from quartz does not change. The profile was made with a precision of 1 μm and pol-

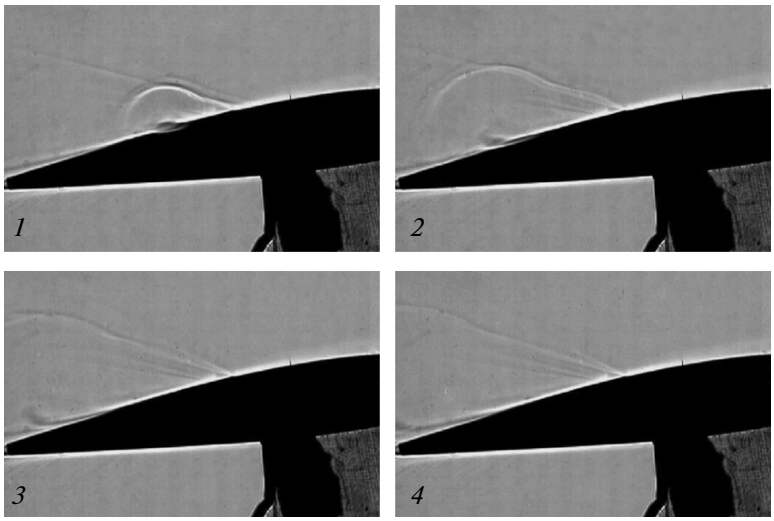

Fig. 1. Dynamics of extended spark discharge on the model surface. Angle of attack is 8 deg. *1*—20 μs, *2*—40 μs, *3*—60 μs, *4*—70 μs after the discharge.

ished. A trapezoidal groove was cut on the upper surface for conducting segments with a length of 5 mm each. Segments were made from Kovar with a coefficient of linear heat expansion smaller by approximately one order of magnitude than that of other grades of steel and other metals. Segments were tightly placed in the groove, and the profile surface on the whole remained smooth. A dielectric Teflon film with a thickness of 50 μm was placed between neighboring segments. High voltage from the accumulation circuit was applied to the end segments.

If the dielectric between several end segments is removed, the discharge gap decreases. The spark length and the value of breakdown voltage also decrease in this case. Experiments with different lengths of the discharge gap (40–120 mm) show that the effective electric field strength equal to the ratio of the voltage at the actuator and the discharge gap between the end segments is constant. This value is 1.0 kV/cm for the following parameters of the supersonic flow: Mach number 2, static flow pressure 0.15 atm. The breakdown mechanism is as follows. If sufficient voltage is supplied to the actuator, gas ionization begins near the nongrounded segment. In this case, the conductivity of the medium between this segment and the neighboring one substantially increases. Since the segments were made from metal, this process was repeated between the next pair of segments in the direction of the grounded segment. When the gas near the actuator surface becomes sufficiently ionized, the main breakdown between the high voltage end segment and the grounded end segment takes place. Oscillograms of discharge current testify that the described process proceeds for no less than 1 μs, which is much smaller than the flight time; therefore, from the point of view of gasdynamic processes, pulsed heating of the medium is instantaneous.

In this case, the electric discharge is independent and occurs when the voltage between the end segments of the discharger reaches a certain value. To study the dynamics of propagation of the flow perturbation caused by the extended spark discharge, it is necessary that the energy of a separate discharge be constant. Using the chosen voltage oscillograms measured within 2 s with a step of 100 ns, it was possible to study fluctuations in breakdown voltage, residual voltage, energy, and repetition rate of electric discharge. Experiment showed that the value of breakdown voltage depends on the angle of attack of the profile, since in the case of change in the angle of attack, the value of static pressure of the flow near the place of discharge initiation changes. In more than 95% of cases, the breakdown voltage is in the range of 9.7–10.1 kV; the value of residual voltage, in the range of 1.5–1.9 kV; and the energy of a separate discharge changes within 10% of the average value, which depends on the capacity of storage condensers. The discharge repetition rate fluctuates to a larger degree; for example, it changes from 5 to 6 kHz, since it depends on the breakdown voltage and regime of operation of the high voltage source. In another case, control with respect to voltage takes place with constant output voltage (about 10 kV). Since the energy of the separate discharge is rather constant (95% of the values lie in the range of 10% of the average value, the distribution halfwidth is 4% of the average value), it is possible to reconstruct the schlieren or shadow picture of the flow from digital frames obtained for different delays between the discharge initiation time and the frame exposure time.

Although heat release using discharge is an instantaneous process, flow perturbations caused by it exist for a time interval sufficient to influence the flow picture. Figure 1 shows the series of shadowgrams of the process of profile streamlining with discharge initiated

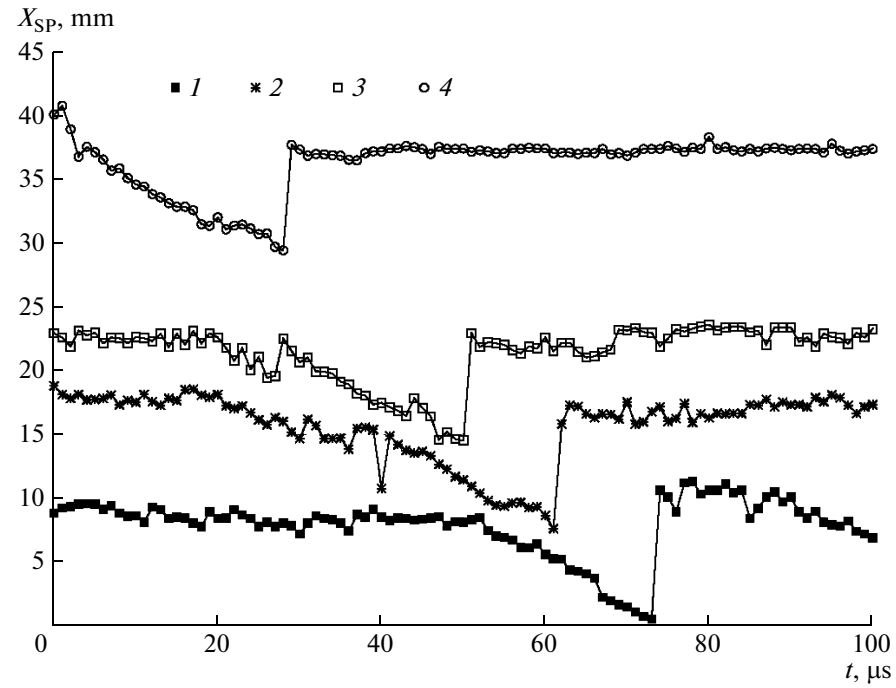

Fig. 2. Position of separation point with respect to the back end of the profile as a function of time after the discharge at different angles of attack: *1*—α = 0°, *2*—α = 8, *3*—α = 10°, *4*—α = 13°.

on the profile surface; only the region of the back edge of the profile is shown. The discharge initiation rate is approximately 5 kHz, the voltage at the actuator is 10.50 kV, the length of the discharge gap is 10.0 cm, the energy of one pulse is 60 mJ, and the discharge time is 300 ns. The frames show weak oblique shocks formed near the actuator due to the surface roughness. Then, downward along the flow, the separation line beginning at a distance of 20 mm from the discharge initiation point can be seen. In the first frame, the shock wave front occurring after discharge initiation can be seen. In subsequent frames, the dynamics of development of gasdynamic perturbation of air flow with time is shown. In essence, the shock wave occurring after the discharge is cylindrical. In frames *2* and *3*, a slight reduction of the separation zone can be seen; on the whole, this improves the aerodynamic characteristics of the profile for the given angle of attack. At a time instant of 70 μs (frame *4*), the action of flow perturbation on the separation zone of the flow terminates and the separation line returns to the initial position. When the process of initiation repeats with a period close to the flow flight time (10^{-4} s), steady-state action on the flow picture can be achieved.

The thus obtained schlieren or shadow pictures of the flow make it possible to obtain the dynamics of interaction of gasdynamic perturbation with the flow separation zone at different angles of attack. Figure 2 shows the position of the separation point as a function of time after the discharge at different angles of attack. The velocity of the cylindrical shock wave occurring after the spark discharge at different discharge energies was also determined. Since the breakdown voltage was constant in experiments, the discharge energy varied with variation in the capacity of storing condensers. The experiment for an angle of attack of 8 deg showed that the change in the discharge energy from 60 to 260 mJ results in growth in the Mach number of the shock wave front from 1.28 to 1.40, respectively, relative to the incident flow. In this case the maximal shift of the separation point caused by the flow perturbation due to the discharge practically does not change.

NUMERICAL SIMULATION

Vortex formation under the action of the thermal source situated near the wall is similar to convective instability. This qualitatively follows from the equation for the flow vorticity,

$$\frac{\partial \mathbf{\Omega}}{\partial t} + (\mathbf{v} \cdot \nabla)\mathbf{\Omega} = \frac{1}{\rho^2}\nabla\rho \times \nabla p + \nu\Delta\mathbf{\Omega}. \qquad (1)$$

The term $\frac{1}{\rho^2}\nabla\rho \times \nabla p$ is the source of vorticity in the nonbarotropic flow, and for the case of thermal action it can be transformed using the expansion of the density gradient,

$$\nabla\rho = \left(\frac{\partial\rho}{\partial T}\right)_p \nabla T + \left(\frac{\partial\rho}{\partial p}\right)_T \nabla p,$$

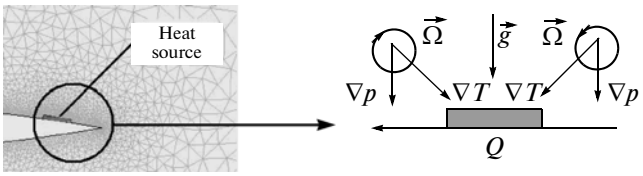

Fig. 3. (Left) Heat source position on the wing, (right) schematic diagram of formation of thermal vortices.

which results in a source of vorticity of thermal nature,

$$\frac{\partial \mathbf{\Omega}}{\partial t} + (\mathbf{V}\cdot\nabla)\mathbf{\Omega} = -\frac{\beta T}{\rho}\nabla \ln T \times \nabla p + \nu\Delta\mathbf{\Omega}, \qquad (2)$$

where the volume expansion coefficient $\beta = \frac{1}{v}\left(\frac{\partial v}{\partial T}\right)_p$, $v = 1/\rho$ is the specific volume.

Vortex formation under thermal action is schematically shown in Fig. 3.

For numerical simulation of convective flow, the NACA0015 wing was used as the aerodynamic profile; the volume heat source was placed on the surface of this wing (Fig. 4).

Steady-state heat release in these calculations was taken equal to $Q = 10$ W/m^2. In the gas at rest (velocity of the incident flow $V_0 = 0$) two vortices with opposite circulation are formed.

The problem was solved in the three-dimensional formulation shown in Fig. 5. The thickness of the boundary layer was determined as $\delta = \sqrt{\nu x/U}$, where ν is the kinematic viscosity of air, x is the distance from the beginning of the aerodynamic body, and U is the velocity of the external flow. The numerical domain was a parallelepiped with finer cells in the boundary layer (24 cells). After the establishment of the flow regime with the given parameters (M = 2, p_0 = 0.1287 atm, $\rho_0 = 0.287$ kg/m^3) of incident gas at a distance of 5 mm from the input, the heat source in the form of a heated plate (length 1 mm, width 0.1 mm) was placed perpendicular to the flow with temperature T = 1000 K (Fig. 5).

The system of continuity equations, equations of motion and energy, and the equation of state was solved in the simulation:

$$\frac{\partial \rho}{\partial t} + \nabla\cdot(\rho\mathbf{v}) = 0,$$
$$\rho\left(\frac{\partial \mathbf{v}}{\partial t} + (\mathbf{v}\cdot\nabla)\mathbf{v}\right) = -\nabla p + \nabla\cdot\boldsymbol{\sigma}, \qquad (3)$$
$$\rho\left(\frac{\partial h}{\partial t} + (\mathbf{v}\cdot\nabla)h\right) = \frac{\partial p}{\partial t} + (\mathbf{v}\cdot\nabla)p + \boldsymbol{\sigma}:\nabla\mathbf{v} + \nabla\cdot(\lambda\nabla T),$$
$$p = \rho RT,$$

where h is the specific enthalpy. Heat conduction and air viscosity as functions of temperature were expressed by the Sutherland formulas,

$$\lambda = \lambda_0\left(\frac{T}{T_0}\right)^{1/2}, \quad \eta = \eta_0\left(\frac{T}{T_0}\right)^{1/2},$$

$\lambda_0 = 2.37\times10^{-2}$ W/(m K), $\eta_0 = 1.82\times10^{-5}$ Pa s, T_0 = 273 K.

Figure 6 shows the pressure distribution in the presence of the heated plate.

It follows from Fig. 7 that the largest vorticity with the opposite circulation is created at the edges of the heated plate (where the temperature gradient is the largest). Downward along the flow vortex, diffusion takes place, which results in their interaction with each other and the flow.

A similar scheme of numerical simulation was used for parameters corresponding to experimental studies; the results demonstrated qualitative agreement of numerical, theoretical, and experimental results.

Experiments on schlieren visualization show that in the case of instantaneous heat release, vorticity Ω described by the following equation occurs in the discharge in the gas flow:

$$\frac{\partial \Omega}{\partial t} + V\frac{\partial \Omega}{\partial x} = \nu\frac{\partial^2 \Omega}{\partial y^2}.$$

This equation is valid for transfer of vorticity in the two-dimensional case when the vector quantity Ω has one nonzero component directed perpendicular to the plane (x, y). In this case when the vorticity is scalar, the considerations for concentration are valid for the

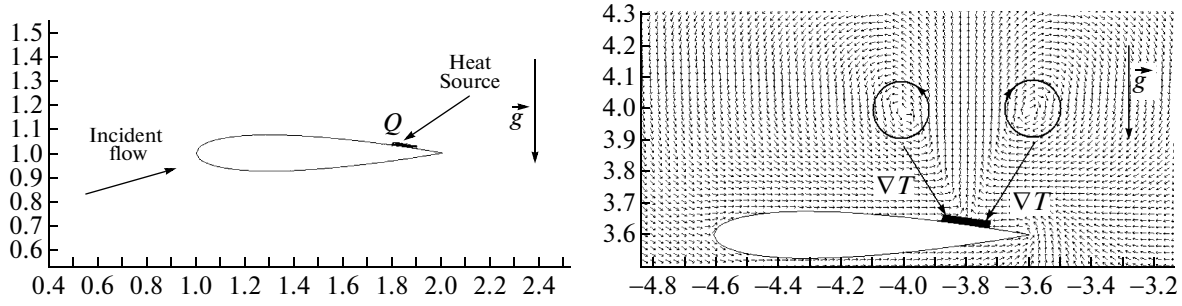

Fig. 4. (Left) Schematic diagram of simulation of convective flow, (right) vector velocity field.

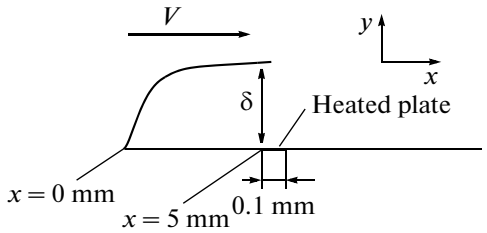

Fig. 5. Schematic diagram of calculation for supersonic flow.

problem of evolution of vorticity created by a point source. For simplicity and pictorial representation, we consider the diffusion equation for concentration c in the one-dimensional case in the absence of convective transfer,

$$\frac{\partial c}{\partial t} = D\frac{\partial^2 c}{\partial y^2},$$

where D is the diffusion coefficient. For the simple problem with a point source and without convective transfer, there exists an analytical solution expressed in terms of the Green's function of the form

$$G(y - y_0, t) = \frac{1}{\sqrt{2\pi Dt}}\exp\left(-\frac{(y - y_0)^2}{2Dt}\right).$$

In the presence of convective transfer, the diffusion equation takes the following form:

$$\frac{\partial c}{\partial t} + V\frac{\partial c}{\partial x} = D\frac{\partial^2 c}{\partial y^2}.$$

To solve this equation, it is necessary to perform the following coordinate transformation:

$$c(t,x,y) = c(t',\xi,y),$$
$$t = t',$$
$$\xi = x - Vt.$$

Then in this case, the solution to the diffusion equation with convective transfer for vorticity is represented in the form of superposition of vorticity of the incident flow and vorticity created by the thermal source,

$$\Omega(t,x,y) = \frac{\partial V}{\partial y} + \Phi_0\delta(x - V(y)t)\frac{1}{\sqrt{2\pi Dt}}\exp\left(-\frac{y^2}{2Dt}\right),$$

where Φ_0 is the vorticity flow through the considered domain of the two-dimensional space. The first term in the equation corresponds to the vorticity of the incident flow, the second one expresses the space–time evolution of vorticity created by the thermal source. In the case of flow separation, the condition of zero vorticity of the incident flow at the separation point is satisfied. An additional source of vorticity results in the fact that the point at which the total vorticity is zero is shifted downward along the flow.

The above theory qualitatively explains the experimentally observed phenomenon of change in the position of the separation point caused by pulsed thermal action.

CONCLUSIONS

The possibility of pulsed-periodic initiation of extended spark discharge on the surface of an aerodynamic body streamlined by a supersonic air flow with a frequency in the kilohertz range and a pulse energy of tens of mJ was experimentally demonstrated. It was shown that if the sectioned discharger is used as the actuator, the effective breakdown of electric field strength is independent of the discharge gap, 1 kV/cm, which is lower by one order of magnitude than the electric strength of air at the same density. In this case, the discharge is formed not only between metallic segments of the actuator, but bridges end segments, forming a homogeneous plasma filament. Single discharge on the surface of the aerodynamic body influences the picture of the streamline during the flight time, and in the case of periodic repetition of discharge initiation in the steady-state case, it can change the parameters of supersonic streamlining. The schematic diagram of numerical simulation was developed, and simulation was performed of the formation of a pair of vortices as a result of impact of the heat source on the supersonic

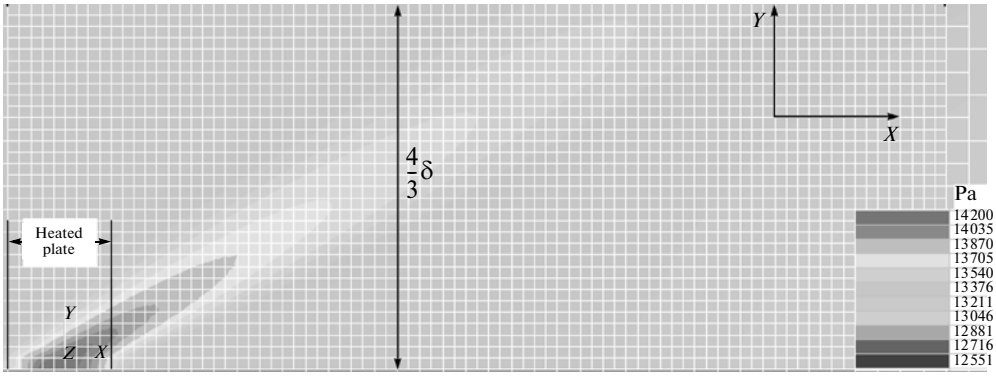

Fig. 6. Pressure distribution.

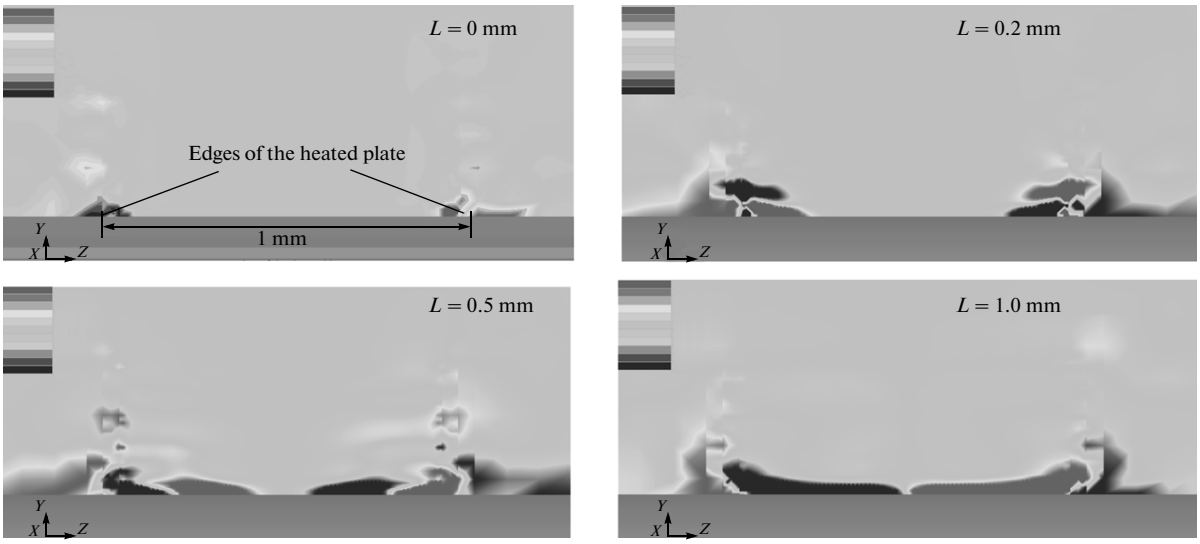

Fig. 7. Distribution of X component of vorticity along the flow at different distances L from the heated plate.

flow with the aerodynamic body. This scheme makes it possible to simulate the action of thermal and plasma actuators on the supersonic flow near the aerodynamic body.

REFERENCES

1. Moreau, E., *J. Phys. D: Appl. Phys,* 2007, vol. 40, no. 3, p. 605.
2. Pavon, S., Ott, P., Leyland, P., Dorier, J.-L., and Hollenstein, Ch., *Proceedings of 47th AIAA Aerospace Science Meeting Including the New Horizons Forum andAerospace Exposition*, Orlando, January 5–8, 2009, AIAA Paper, p. 1.
3. Golub, V.V., Saveliev, A.S., Sechenov, V.A., and Son, E.E., *Proceedings of 47th AIAA Aerospace Science Meeting Including the New Horizons Forum and Aerospace Exposition*, Orlando, Florida, January 4–7, 2010, AIAA Paper, p. 10.
4. Aksenov, V.S., Golub, V.V., Gubin, S.A., et al., *Pis'ma Zh. Tekh. Fiz.,* 2004, vol. 30, no. 20, p. 1.
5. Vasil'ev, L.A., *Tenevye metody* (Direct Shadow Methods), Moscow: Nauka, 1968.
6. Yan, H., Gaitonde, D., and Shang, J., *38th AIAA Plasmodynamics and Lasers Conference*, Miami, Florida, AIAA-2007-3877, 2007.
7. Yan, H., Gaitonde, D., and Shang, J., *45th AIAA Aerospace Science Meeting and Exibit*, Reno, Nevada, AIAA-2007-1234USA, 2007
8. Yan, H. and Gaitonde, D., *39th Plasmadynamics and Lasers Conference,* Seattle, Washington, AIAA-2008-3790, 2008.
9. Ya, H. and Gaitonde, D., *47th AIAA Aerospace Science Meeting*, Orlando, January 5-8, AIAA-2009-923, 2009.
10. Son, E.E. and Tereshonok, D.V., *47th AIAA Aerospace Science Meeting*, Orlando, January 5-8, AIAA-2009-844, 2009.
11. Joslin, R.D. and Grosch, C.E., *Phys. Fluids,* 1995, vol. 7, p. 3042.
12. Narayanaswamy, V., Clemens, N.T., Laxminarayan, L.R., Investigation of a Pulsed-Plasma Jet for Shock/Boundary Layer Control, *48th AIAA Aerospace Sciences Meeting Including the New Horizons Forum and Aerospace Exposition 4–7 January 2010*, Orlando, Florida, AIAA-paper 2010-1089.
13. Caraballo, E., Webb, N., Little, J., Kim, J-H., and Samimy, M., "Supersonic Inlet Flow Control Using Plasma Actuators," AIAA-2009-724, 2009.